DOI: 10.26599/FSHW.2025.9250521

Contents lists available at SciOpen

Food Science and Human Wellness

journal homepage: https://www.sciopen.com/journal/2097-0765

China Food Publishing Co.

Lactiplantibacillus plantarum TXZ 2-35 Protects Mice Against Ulcerative Colitis by Inhibiting Ferroptosis and Regulating of Intestinal Microbiota and Lipid Metabolites

Luyao Liu[1], Dandan Han[2], Huan Liu[3], Fan Zhao[4], Xin Lü[1], Gang Wu[1*], Yanglei Yi[1*]

[1]*College of Food Science and Engineering, Northwest A&F University, Yangling, 712100, Shaanxi Province, China*

[2]*Shaanxi Yiruikang Biotechnology Co., LTD, Xianyang, 712023, Shaanxi Province, China*

[3]*Department of Emergency, Ruijin Hospital, Shanghai Jiao Tong University School of Medicine, 197 Ruijin Er Road, Shanghai, 200025, China*

[4]*College of Animal Science and Technology, Northwest A&F University, Yangling，712100, Shaanxi Province, China*

ABSTRACT: Ferroptosis, a newly recognized type of regulated cell death associated with intestinal epithelial dysfunction, can influence the onset and severity of inflammatory bowel disease (IBD). Thus, there is growing interest in the novel therapy targeting ferroptosis for the treatment of IBD. Here, we investigated the effects of dietary supplementation with viable *Lactiplantibacillus plantarum* TXZ 2-35 on dextran sodium sulfate (DSS)-induced ulcerative colitis in mice. The results revealed that the disease severity was alleviated by *L. plantarum* TXZ 2-35 as evidenced by increased body weight, colon length and decreased disease activity index (DAI). Moreover, the levels of inflammation-related cytokines (TNF-α, IL-1β, IL-6) in serum and oxidative enzymes (MPO) in the colon were downregulated by *L. plantarum* TXZ 2-35 supplementation. Interestingly, transcriptomic data revealed that ferroptosis related genes were significantly enriched after TXZ 2-35 supplementation. In addition, TXZ 2-35 restored morphological changes and attenuated the iron content in the colon, accompanied by increased Glutathione Peroxidase (GSH) and decreased Malondialdehyde (MDA), which all together proved that *L. plantarum* TXZ 2-35 suppressed ferroptosis in colonic epithelial cells. We then sought to determine whether gut microbiota and its metabolites played a role in the process of ferroptosis changing. The results showed that TXZ 2-35 enhanced the abundance and diversity of beneficial bacteria such as Ruminococcus_1, Lachnospiraceae_NK4A136_group, and Anaeroplasma, while reducing levels of Dubosiella. Correlation analysis showed that the the decreased level of PL-PUFAs, gut microbiota metabolite, may be the cause of ferroptosis. In conclusion, our study indicates that TXZ 2-35 has strong potential as a therapeutic adjuvant for ulcerative colitis, through regulating gut microbiota and the metabolite and therefore decreasing ferroptosis.

Keywords: ferroptosis, gut microbiota, PL-PUFAs, *Lactobacillus plantarum*, ulcerative colitis，inflammatory bowel disease

1. Introduction

Inflammatory bowel disease (IBD), consisting of Crohn's disease (CD) and ulcerative colitis (UC), is a chronic relapsing condition[1].Patients with IBD are at increased risk of developing colorectal cancer

***Corresponding author**
gang.wu@nwsuaf.edu.cn (G. Wu); yyi@nwafu.edu.cn (Y. Yi)

Received 20 August 2024
Received in revised from 28 October 2024
Accepted 9 January 2025

(CRC)[2]. IBD pathogenesis is associated with gut mucosal inflammation, epithelial damage, and dysbiosis[3]. Dysbiosis consists of the disturbances of gut microbiota and microbiota-derived metabolites[4]. Probiotics are live microorganisms that confer beneficial effects on gut microbiota in sufficient doses. Probiotics are widely used in the adjuvant treatment of diseases due to their efficacy and safety. Recent studies have shown that probiotics improve the symptoms of both colitis animal models and IBD patients, showing great potential in the treatment of IBD[5-7]. However, the mechanisms of action of specific probiotics remain unclear.

Ferroptosis is a type of programmed cell death driven by iron-dependent lipid peroxidation, primarily produced through the free iron–induced Fenton reaction and oxidized phospholipid (PL)-containing polyunsaturated fatty acids (PL-PUFAs)[8]. Additionally, the pathological involvement of ferroptosis has been demonstrated in patients with UC[9-10]. Previous studies have shown that elevated iron deposition, glutathione (GSH) depletion, glutathione peroxidase 4 (GPX4) inactivation and lipid peroxidation, and mitochondrial disruption are key features in ferroptosis[11]. Mechanistically, lipid metabolism—particularly that of PL-PUFAs, plays a critical role in regulating ferroptosis[12]. Two key genes are involved in lipid peroxidation regulation, ACSL4 catalyzes the conversion of free PUFAs to acyl-CoA derivatives (PUFA-CoAs), which can be further catalyzed by lysophosphatidylcholine acyltransferase 3 (LPCAT3) to produce PL-PUFAs.

Microbiota and its metabolites are reported to be involved in ferroptosis. Gut microbial metabolites can be divided into two categories based on their functions: One that inhibits ferroptosis and the other that promotes it. *Trans*-3-indoleacrylic acid (IDA) and Daidzein inhibited the ferroptosis[13-14] while Arachidonic acid (AA) and glycochenodeoxycholate (GCDCA) facilitated the ferroptosis[15-16]. The essential role of lipid-based gut microbial metabolites to ferroptosis is evident but far from fully understood[17]. In addition, the effects of probiotics vary and depend on type and dose as well as on their interaction with the host in different ways. One of the theorized mechanisms of probiotic action is the regulation of lipid metabolism[18]. *L. plantarum* TXZ 2-35 exhibits favorable probiotic characteristics, including good tolerance to acid and bile salts, antibiotic sensitivity, strong adhesion to intestinal cells, and antioxidant properties in our previous study, therefore it was selected to investigate its underlying mechanisms of action[19]. We hypothesized that the attenuation of UC by TXZ 2-35 is mediated primarily through the regulation of gut microbiota dysbiosis and related lipid metabolites, thus inhibiting ferroptosis.

In this study, the alleviating effect of oral administration of *L. plantarum* TXZ 2-35 targeting ferroptosis was tested in a murine model of dextran sulfate sodium (DSS)-induced colitis. Initially, we investigated the ameliorative effects of oral TXZ 2-35 on colitis in mice. Moreover, significant ferroptosis was observed in the colonic epithelial cells of DSS-induced colitis mice, and oral administration of TXZ 2-35 inhibited the development of ferroptosis. To further establish the link between ferroptosis and TXZ 2-35 administration, we applied the ferroptosis inhibitor Fer-1 and the ferroptosis inducer ferric citrate, along with TXZ 2-35, to treat ulcerative colitis (UC), assessing its effect on suppressing ferroptosis.

Additionally, to investigate the potential mechanisms behind the regulatory effects of oral TXZ 2-35 on DSS-induced colitis, we investigated the intestinal microbiota and its metabolites in mice using 16S rRNA sequencing and untargeted lipidomics. These findings revealed for the first time that *L. plantarum* TXZ 2-35 protects mice from experimental ulcerative colitis by targeting ferroptosis through the regulation of intestinal microbiota and lipid metabolites, providing novel insights into the probiotics regulation of the ferroptosis for UC.

2. Materials and methods

2.1 Bacterial cultures

L. *plantarum* TXZ 2-35 (CGMCC No. M 20232009) isolated from traditional dairy products in western China was grown in MRS broth medium. The inoculated medium was incubated at 37℃ under aerobic conditions for 24 hours. The bacteria were cultured to an optical density (OD) of 1.2, corresponding to a concentration of 4×10^{11} colony-forming units (CFU) per milliliter. Afterward, the bacteria were pelleted by centrifugation at 4℃ for 10 min at 5,000 × g. The bacterial cells were then resuspended in sterile saline. The viable bacterial suspensions were prepared freshly before every use.

2.2 Cell Culture and Ferroptosis Assay

H1299 cells were purchased from the National Science and Technology Infrastructure (Shanghai, China). H1299 cells were cultured in RPMI 1640 medium with 10% FBS according to the American Type Culture Collection guidelines. 0.5 μmol/L RSL3 was used in H1299 cells for 6 hours, according to previous studies[20]. Then the cell-free extract of *L. plantarum* TXZ 2-35 was used at various concentrations to evaluate ferroptosis by measuring cell viability. Cells were collected after TXZ 2-35 treatment and subjected to viability, lipid ROS and Western blot analyses.

H1299 cells were seeded in 96-well plates at a concentration of 5×10^3 cells per well, cell viability was measured using a CCK-8 kit according to the manufacturer's instructions. Briefly, 10 μL of reagent was added to each well and incubated at 37 ℃ for 2−3 h. The plates were then scanned at 450 nm using a plate reader (TECAN, Spark).

Lipid ROS were measured according to the manufacturer's instructions. Briefly, cells were incubated in 6-well plates and treated with either PBS or *L. plantarum* TXZ 2-35 for 20 hours. Cells were then incubated with lipid ROS indicator BODIPY 581/591 C11 dye at 37 ℃ for 30 min and washed twice with PBS. Fluorescence intensity was monitored by flow cytometry (BD FACSAria III).

Cells were harvested and suspended in Radio Immune Precipitation Assay buffer on ice for 30 min. Proteins were separated by sodium dodecyl sulfate-polyacrylamide gelelectrophoresis (SDS-PAGE) and transferred onto nitrocellulose membranes (0.45 μmol/L, GE). The membranes were probed with the primary and secondary antibodies. The primary antibody used were: GAPDH, Nrf2, GCLC, SLC7A11, HO-1, NQO1, GPX4, CAT, SOD1 and SOD2 (Cell Signaling Technology). The anti-Flag and secondary antibodies were obtained from Sigma-Aldrich. After overnight incubation with a primary antibody, the

membranes were incubated with horseradish peroxidase-conjugated secondary antibody at room temperature for 1 h. Finally, the proteins were detected using an imaging system (Bio-Rad, Hercules, CA). ImageJ software was used to quantify protein abundance.

2.3 Animals and induction of colitis

Male C57BL/6J mice (6 weeks old, approximately 20g) were purchased from Tengxin Biotechnology Co. (Chongqing, China). All mice were provided with water and food ad libitum, and were housed in an animal room at standard conditions (temperature, 21℃–24℃; humidity, 45%–60%; 12-hour light/dark cycle). Dextran sulfate sodium (DSS)(molecular mass 36–40 kDa, MP Biologicals, Solon, OH, USA) was dissolved in the drinking water at a concentration of 2.5% (wt/vol) for 7 days to induce colitis. Mice were monitored daily for survival, general appearance, body weight, stool consistency, and rectal bleeding. Disease activity index (DAI) was evaluated using the method described previously[21].

2.4 Treatments and sample collection

All experimental procedures were approved by Animal Experiment Ethics Committee of Northwest Agriculture and Forestry University (XN 2023-0721). Groups of ten mice were anesthetized, and blood samples were collected from the retro-orbital venous plexus with a glass capillary. Mice were then sacrificed and the colon was immediately excised to measure its length (between the proximal rectum and the ileocecal junction). Besides, approximately 1 cm of proximal colon tissue was collected for histological examination and transmission electron microscopy (TEM) observation. The remaining colon tissue were stored at −80℃ for further analysis. Cecal contents were also collected and stored at −80℃.

Experiment 1

DSS-induced colitis was induced following previously described methods with some modifications[22]. The experimental design is shown in **Fig. 1A**. After acclimation for 7 days, the mice were randomly divided into three groups (n = 10): Control (Con), DSS -induced colitis (DSS) and pretreatment with TXZ 2-35 (TD). The Con group received normal tap water and was gavaged with 200 μL of sterile saline daily. The DSS group was gavaged with 200 μL of sterile saline daily and received 2.5% DSS in the last 7 days. The TD group received 16 days of viable TXZ 2-35 (4×10^{11} CFU/mL, 200μL per day for each mouse, dissolved in 2 mL saline) intervention via intragastric gavage and 2.5% DSS in the last 7 days.

Experiment 2

The experimental design is shown in **Fig. 3A**. The mice were randomly divided into five groups DSS, FD, TFD, RD, TRD. All five groups received 2.5% DSS in water for the last 7 days. The FD group received Ferric citrate (15mg/kg, B5291, Shanghai Macklin Biochemical Technology Co., Ltd) by vail tail injection, the RD group received Fer-1 (1mg/kg/d, S7243, Selleck Biotechnology Co., Ltd) by intraperitoneal injection for the last 7 days, and were also gavaged with 200 μL of sterile saline daily. The TFD and TRD groups received 200 μL of viable TXZ 2-35 (4×10^{11} CFU/mL) daily via gavage and the other procedures are the same as the FD and RD groups. The doses of Fer-1 and Ferric citrate were based on previous methods[23-24].

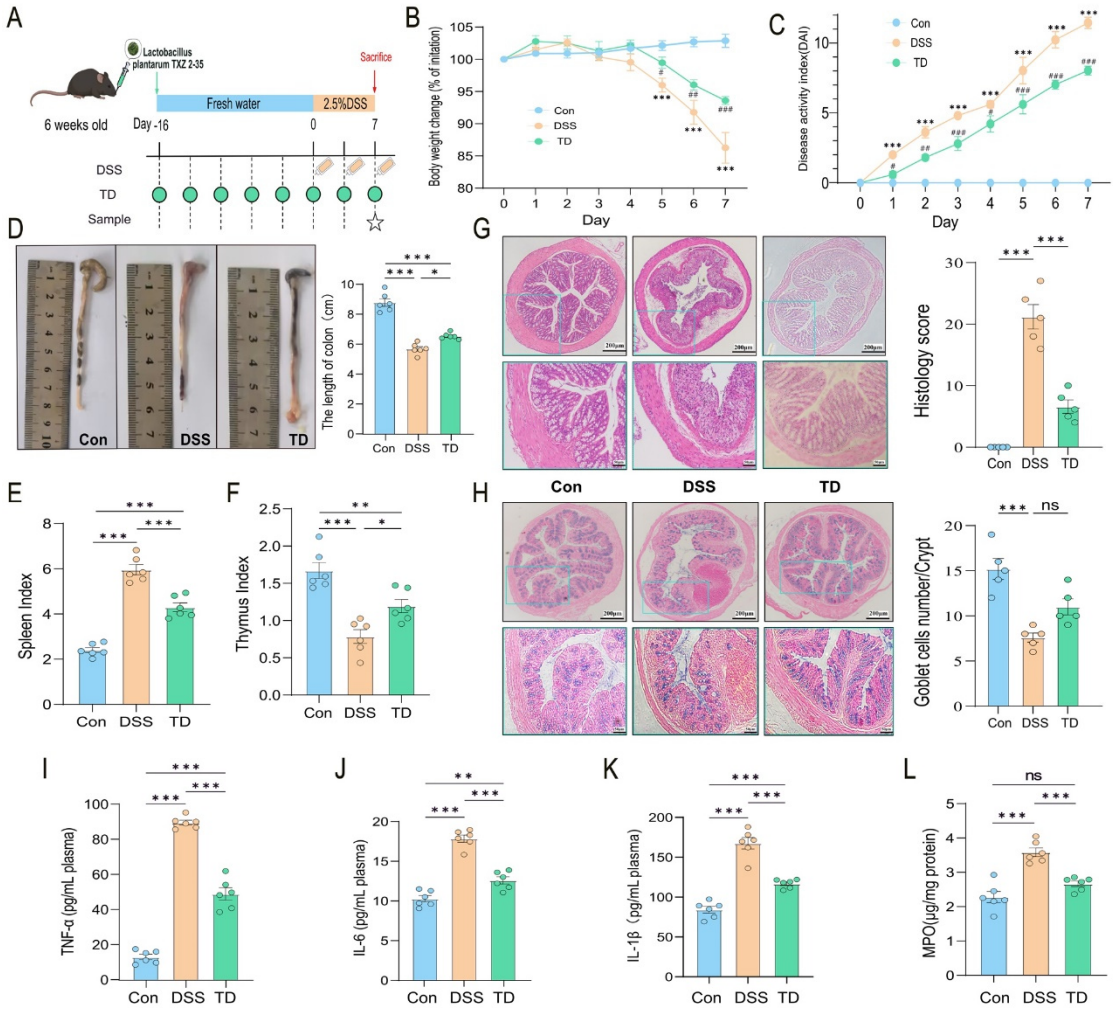

Fig 1 *L.plantarum* TXZ 2-35 improved the pathological phenotype of DSS-induced colitis in mice. (A) Experimental protocol for DSS-induced colitis in mice and probiotic intervention. (B)Percentage change in body weight (%) in different groups and (C) Disease activity index (DAI) scores for all treated mice after DSS administration. Statistical significance was determined using two-way ANOVA, followed by Tukey test. *P≤0.05, **P≤0.01, ***P≤0.001 is DSS relative to Control group, #P≤0.05, ##P≤0.01, ###P≤0.001 is TD relative to DSS group. (D) Macroscopic observation (left) and colon length (right) on the final day. (E,F) Ratios of spleen weight to body weight and thymus weight to body weight. (G) Representative images of H&E staining (left) and histology scores (right) of colon tissues. (H) Representative images of Alcian blue staining (left) and goblet cell counts (right) in colon tissues (scale bar: 500 μm and 50 μm). (I) Serum levels of TNF-α, (J) IL-1β and (K) IL-6. (L) Concentration of MPO in colon tissues. Data were shown as mean ± SEM. Statistical significance was determined using one-way ANOVA, followed by Tukey test. ns. means not significant, *$P < 0.05$, **$P < 0.01$, ***$P < 0.001$.

2.5 Histological analysis

Colons were fixed in 4% paraformaldehyde, and embedded in paraffin. Five-μm-thick tissue sections were stained with hematoxylin and eosin (H&E) for light microscopic examination using a DP73 light microscope (Olympus, Tokyo, Japan). Colonic tissues were sectioned at 5 μm thickness, deparaffinized and stained using Alcian Blue staining kit (Leagene, Beijing, China) according to the manufacturer's instructions. The colonic mucosa damage score was assessed as previously described[25].

2.6 TEM analysis

The colons were washed with precooled PBS (pH 7.4), then cut into small pieces and incubated overnight in 0.1 M PBS (pH 7.4) containing 2.5% glutaraldehyde. Selected areas of the intestines were

postfixed in 1% osmium tetroxide for 1 hour, dehydrated in a graded ethanol series, and embedded in epoxy resin. Polymerization was performed at 80 ℃ for 24 hours. Ultrathin sections (100 nm) were cut, stained with uranyl acetate and lead citrate, and viewed under a TEM (HT7800, Tokyo, Japan).

2.7 Enzyme-linked immunosorbent assay

The serum levels of TNF-α, IL-1β and IL-6 were quantified using the corresponding commercial ELISA kit (Shanghai Enzyme Linked Biotechnology Co., Ltd, Shanghai, China). Colonic tissues were homogenized in phosphate-buffered saline (pH 7.4) and centrifuged at 12,000g for 10 minutes at 4℃. Then the supernatants were collected for the measurement of protein concentrations and below index. The colon tissue protein was quantified using a bicinchoninic acid (BCA) protein assay kit (Zhonghui Hecai Biomedical Technology Co. Ltd., Shaanxi, China). While the myeloperoxidase (MPO) activity, the representative redox enzymes Malondialdehyde (MDA), Glutathione Peroxidase (GSH) and tissue iron content were measured using a corresponding commercial ELISA kit (Jiancheng Bioengineering Institute, Nanjing, China). The ATP detection kit (S0026, Beyotime) was used to detect the level of ATP in colon tissues. All procedures were performed according to the manufacturer's instructions.

2.8 The 16S gene sequencing and analysis

To further discover the influence of TXZ 2-35 to mice gut microbiota, The fecal microbiota composition was analyzed by 16S sequencing. Fecal samples from six mice per group were randomly collected and stored at −80℃. Microbial genomic DNA was isolated with PowerSoil DNA isolation kit (MoBio Laboratories Inc., Carlsbad, USA) by following manufacturer’s instructions. PCR amplicons of the 16S rRNA region were amplified and sequenced using an Illumina MiSeq platform with the paired primers targeting V3-V4 regions 338F(: 5’-ACTCCTACGGGAGGCAGCA -3’) and 806R(: 5’-GGACTACHVGGGTWTCTAAT-3’). Sequencing libraries were generated using NEBNext® Ultra™ II DNA Library Prep Kit for Illumina® (New England Biolabs, MA, USA) following manufacturer's recommendations and index codes were added. The library quality was assessed on the Qubit@ 2.0 Fluorometer (Thermo Fisher Scientific, MA, USA). At last, the library was sequenced on an Illumina Nova6000 platform. Operational Taxonomic Units (OTU) method was UPARSE. Cecal microbiota diversity, including Chao1 and Shannon indices, was analyzed using the vegan package in R software (version 4.3.1). The relative abundance of the phyla and genus of the intestinal microbiota was analyzed by the Kruskal-Wallis test after multiple comparison adjustment by the Benjamini & Hochberg method. To evaluate the difference in heterogeneous community structure between the experimental groups, principal coordinate analysis was performed based on weighted Unifrac distances of Bray-Curtis dissimilarity using the vegan package, followed by adonis analysis. Differential abundance analysis was performed to assess variations in taxonomic abundances between groups using the Welch’s t-test of STAMP (version 2.1.3). Spearman’s correlation coefficient was computed to analyze the relationship between the lipid metabolites and microbes using the stats package.

2.9 RNA sequencing and data analysis

Total RNA was isolated using the TRIzol (Kangwei,model:CW0580S). The concentration of extracted RNA was detected with Nanodrop2000, (manufacturer:Thermo, model: Nanodrop2000), and the integrity was detected with Agient2100, LabChip GX (manufacturer and model:Perkin Elmer LabChip GX).The library preparation of cDNA, and Next Generation Sequencing (PE150) was performed using Hieff NGS Ultima Dual-mode mRNA Library Prep Kit for Illumina (Yeasen, model:13533ES96), and Illumina NovaSeq6000 with NovaSeq 6000 S4 Reagent Kit (San Diego), respectively. Reads were first trimmed to remove the adapter sequence and read quality was checked using fastp. Transcripts were quantified and mapped to the indexed mouse genome (M23, GRCm38) using Salmon. Transcript-level quantification was then summarized to the gene level, annotated, and prepared for differential gene expression analysis using the R package tximeta. The R/Bioconductor package DESeq2 was then used to identify differentially expressed genes in each condition using a Benjamini-Hochberg test adjusted for false discovery rate[26].

2.10 Lipidomic analyses

Fifity mg fecal sample was mixed with 280 μL methanol:water (2:5, v/v) solution and 400 μL Methyl Tert-butyl Ether (MTBE) in a 2-mL microtube. Samples were then homogenated at -10 ℃ by High throughput tissue crusher Wonbio-96c (Shanghai wonbio technology co., LTD., Shanghai, China) operating at a frequency of 50 Hz for 6 min, then followed by sonicated at 40 kHz for 30 min at 5℃. Subsequently, the samples were placed at -20℃ for 30 min, followed with centrifugation at 13,000g at 4℃ for 15 min. Lipid extracts (350 μL) in the upper phase were transferred to new tubes and evaporated to dryness under a gentle stream of nitrogen. For UHPLC-MS/MS analysis, the samples were reconstituted in 100 μL loading solution of isopropanol : acetonitrile (1:1, v/v) by sonication (40KHz) in a 5℃ water bath. Extracted lipids were spun for 15 min at 13,000g at 4℃ and 2 μL supernatant were used for analysis. The mass spectrometric data was collected using a Thermo UHPLC-Q-Exactive HF-X Benchtop Orbitrap Mass Spectrometer equipped with a heated-electrospray ionization (HESI) source operating in positive and negative ion mode. Data acquisition was performed with the Data Dependent Acquisition (DDA) mode. The detection was carried out over a mass range of 200-2000 m/z.

The data were analyzed through the free online platform of majorbio choud platform (cloud.majorbio.com). Lipidomic features detected at least 80% in any set of samples were retained. After filtering, minimum metabolite values were imputed for specific samples in which the metabolite levels fell below the lower limit of quantitation and each Metabolic features were normalized by sum. In order to reduce the errors caused by sample preparation and instrument instability, the response intensity of the sample mass spectrum peaks was normalized by the sum normalization method, and the normalized data matrix was obtained. At the same time, variables with relative standard deviation (RSD) > 30% of QC samples were removed, and log10 logarithmization was performed to obtain the final data matrix for subsequent analysis.

Perform variance analysis on the matrix file after data preprocessing. The R package ropls (Version 1.6.2) performed principal component analysis (PCA) and orthogonal least partial squares discriminant

analysis (OPLS-DA), and used 7-cycle interactive validation to evaluate the stability of the model. In addition, student's t-test and fold difference analysis were performed. The selection of significantly different metabolites was determined based on the Variable importance in the projection (VIP) obtained by the OPLS-DA model and the p-value of student's t test, and the metabolites with VIP>1, $P < 0.05$ were significantly different metabolites.

2.11 Statistical analysis

All data were expressed as the means ± standard error of the mean (SEM) from≥6 independent experiments. All statistical analyses were performed using GraphPad Prism software (version 9.0) and R tools (version 4.3.1). For comparisons involving more than two groups, one-way or two-way ANOVA was used, followed by Tukey's multiple comparisons test. The Spearman's correlation analysis was used to establish the connection between the altered fecal microbes and fecal lipid metabolites. Differences were considered statistically significant when P value was <0.05. The graphical abstract was using Figdraw (version 2.0).

3. Results

3.1 L. plantarum TXZ 2-35 Alleviated the Severity of DSS-Induced Colitis in Mice

The colitis mouse model was induced by administering 2.5% DSS in drinking water for 7 days. Mice received daily oral gavage of either 4×10^{11} CFU/mL TXZ 2-35 or saline for the first 16 days(**Fig. 1A**). The colitis model was successfully established, as evidenced by markedly increased body weight loss (**Fig. 1B**), Disease Activity Index (DAI)—a combined score of body weight loss, stool consistency, and rectal bleeding (**Fig. 1C**) and colon shortening (**Fig. 1D**), spleen swollen (**Fig. 1E**), thymus shrinkage (**Fig. 1F**). In the treatment group with TXZ 2-35 supplementation, these symptoms were alleviated. To examine the effects of TXZ 2-35 on colon structure, we assessed the colonic mucosal barrier and mucin-secreting goblet cells in the colonic epithelium using H&E staining and Alcian blue staining. Histological score was increased in the colon tissue of DSS-induced colitis mice, confirmed by the intestinal barrier damage, containing inflammatory infiltrated, crypt damage and alteration of epithelial and mucosal structure, while these effects could be alleviated by the supplement of TXZ 2-35(**Fig. 1G**). DSS treatment also resulted in a reduced number of Alcian blue-positive (goblet) cells, whereas TXZ 2-35 treatment improved the number of goblet cells(**Fig. 1H**). As previously reported, DSS induces both systemic and intestinal inflammatory responses[27]. Serum concentrations of TNF-α (**Fig. 1I**), IL-6 (**Fig. 1J**), IL-1β (**Fig. 1K**) and colonic concentrations of MPO (**Fig. 1L**) were increased in DSS-induced mice, while TXZ 2-35 supplementation reduced the concentration of these indices thereby alleviating inflammation. Collectively, these data indicated that TXZ 2-35 supplementation ameliorates DSS-induced colitis in mice.

3.2 L. plantarum TXZ 2-35 Ameliorated DSS-Induced Ferroptosis in Mice Colonic Epithelial Cells

Previous studies have demonstrated that colonic epithelial cells, both in humans and mice, undergo ferroptosis when colitis is induced[28-29]. This phenomenon was also observed in our results, as indicated by

Figure 2A, where smaller mitochondria, increased membrane density, and decreased mitochondrial cristae were noted in the DSS group. Supplementation with *L. plantarum* TXZ 2-35 has the potential to suppress the occurrence of ferroptosis, as TXZ 2-35 supplementation partly restored the morphological changes in colonic epithelial cells (**Fig. 2A**). To confirm that ferroptosis was indeed involved in the ameliorative effects of TXZ 2-35 on colitis in mice, we further measured typical ferroptosis indices, including malondialdehyde (MDA), glutathione (GSH) levels, iron content and ATP levelss in the colonic tissues. The results showed that mice with colitis had significantly lower concentrations of glutathione (GSH) and ATP, as well as elevated malondialdehyde (MDA) and iron levels. Interestingly, these indices were notably altered by TXZ 2-35 supplementation, with treated mice exhibiting increased GSH levels and ATP levels, decreased MDA and iron concentrations (**Fig. 2B-E**). Collectively, these results suggest that TXZ 2-35 effectively mitigates the ferroptosis associated with colitis.

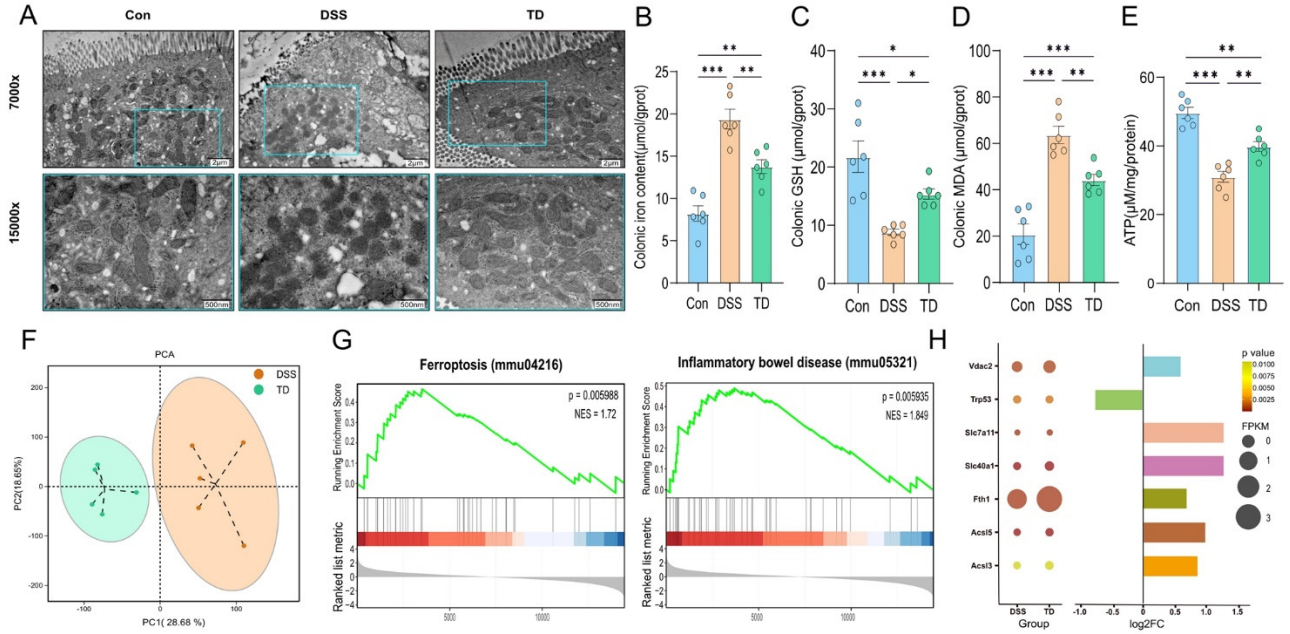

Fig 2 *L. plantarum* TXZ 2-35 inhibited the development of ferroptosis in colonic epithelial cells in mice. (A) Representative transmission electron micrographs of colonic epithelial cells (scale bar: 500 μm and 50 μm). (B) Concentration of iron, (C) GSH, (D) MDA and (E) ATP in colon tissues. (F) Principal Component Analysis (PCA) plot of colon tissues from DSS and TD groups based on transcriptome analysis. (G) Gene set enrichment analysis (GSEA) of the ferroptosis pathway and the inflammatory bowel disease pathways.(H) Left: bubble plot showing the normalized expression of ferroptosis marker genes in the mice colon. Right: bar plot illustrating the regulation of the ferroptosis marker genes by supplementation with *L. plantarum* TXZ 2-35. Data were shown as mean ± SEM. Statistical significance was determined using one-way ANOVA, followed by Tukey test. ns. not significant, *$P < 0.05$, **$P < 0.01$, ***$P < 0.001$.

To explore the host response to TXZ 2-35 supplementation, transcriptome analysis was performed using the colon tissue. As shown in **Fig. 2F**, the Principal Coordinates Analysis (PCoA) using differentially expressed genes (DEGs) revealed distinct clustering between the DSS group and the TXZ 2-35 (TD) group. Gene Set Enrichment Analysis (GSEA) results indicated that TXZ 2-35 supplementation suppressed ferroptosis and inflammatory bowel disease (IBD)-related genes in colitis mice (**Fig. 2G**). Additionally, it affected pathways related to fat digestion and absorption, the biosynthesis of unsaturated fatty acids, and genes associated with cholesterol metabolism (**Fig. S1**). Interestingly, several reported ferroptosis-associated genes, namely, voltage-dependent anion channel 2 (Vdac2), acyl-CoA synthetase long-chain family member

3 (Acsl3), acyl-CoA synthetase long-chain family member 5 (Acsl5), solute carrier family 40 member 1 (Slc40a1), transformation related protein 53 (Trp53), solute carrier family 7 member 11 (Slc7a11), and Ferritin Heavy Chain 1(Fth1), all of which participate in the regulation of lipid or iron metabolism[30-32] were significantly altered after the supplementation of TXZ 2-35 in our study (**Fig. 2H**). The transcriptomic results indicated that ferroptosis involved in colitis while the TXZ 2-35 supplementation regulated the genes expression related to ferroptosis.

3.3 Inhibition of Ferroptosis Alleviated DSS-Induced Colitis in Mice

To explore the role of ferroptosis in colitis, a ferroptosis inhibitor (Fer-1, RD group) and a ferroptosis inducer (ferric citrate, FD group) were administered to mice via intraperitoneal and tail vein injections during the DSS-induced colitis period, specifically during the last 7 days of the experiment. Simultaneously, TXZ 2-35 were supplemented to both the RD and FD groups, resulting in the TRD (TXZ 2-35+RD) and TFD (TXZ 2-35+FD) groups (**Fig. 3A**). The results demonstrated that treatment with ferric citrate (FD group) worsened colitis symptoms, whereas intraperitoneal injection of Fer-1 alleviated these symptoms, confirming the crucial role of ferroptosis in the development of colitis. TXZ 2-35 supplementation significantly mitigated the symptoms induced by ferric citrate but did not provide additional relief when the ferroptosis inhibitor Fer-1 was already administered. This was evident from measurements of body weight loss (**Fig. 3B**), Disease Activity Index (DAI) (**Fig. 3C**), colon length (**Fig. 3D**), as well as spleen and thymus indices (**Fig. 3E**). Histological analysis confirmed the ameliorating effects of TXZ 2-35 and Fer-1 on colitis, showing reduced mucosal erosions and decreased inflammatory infiltrations (**Fig. 3F&G**). Both TXZ 2-35 and Fer-1 significantly reduced the thickness of the colonic epithelial mucosa, desirably increased the number of goblet cells, and restored the mucosa to a more normal state (**Fig. 3H&I**). Furthermore, transmission electron microscopy (TEM) observation of intestinal epithelial cells (IECs) displayed the typical subcellular morphological characteristics of ferroptosis in response to DSS, including cell membrane vesicles or ruptures, smaller or shriveled mitochondria, and decreased or disappeared mitochondrial cristae. Both oral TXZ 2-35 and treatment with Fer-1 protected the decrease of number of globlet cells and ATP levels in DSS-induced colitis (**Fig. 3J&K**).

Pro-inflammatory cytokines in the plasma and colon were measured. Plasma concentrations of TNF-α (**Fig. 3L**), IL-6 (**Fig. 3M**), and IL-1β (**Fig. 3N**), as well as colon concentrations of MPO (**Fig. 3O**), were dramatically increased by ferric citrate but decreased in colitis mice in response to TXZ 2-35 and Fer-1 treatment. Remarkably, malondialdehyde (MDA), an important product of lipid peroxidation, was increased in colitis mice treated with ferric citrate, indicating heightened oxidative stress. Both oral supplementation with TXZ 2-35 and treatment with Fer-1 were able to reduce the levels of MDA (**Fig. 3P**), demonstrating their effectiveness in mitigating lipid peroxidation. In addition, the colonic levels of iron were dramatically decreased, while GSH levels were increased in response to TXZ 2-35 and Fer-1 (**Fig. 3Q&R**). These results collectively indicate that the ferroptosis inducer ferric citrate exacerbated colitis symptoms, while oral TXZ 2-35 was capable of suppressing the effects of ferric citrate by reducing ferroptosis. Similarly, Fer-1

alleviated colitis in mice by inhibiting ferroptosis. Combining TXZ 2-35 with Fer-1 did not enhance the therapeutic effects, as both treatments target the same ferroptosis pathway.

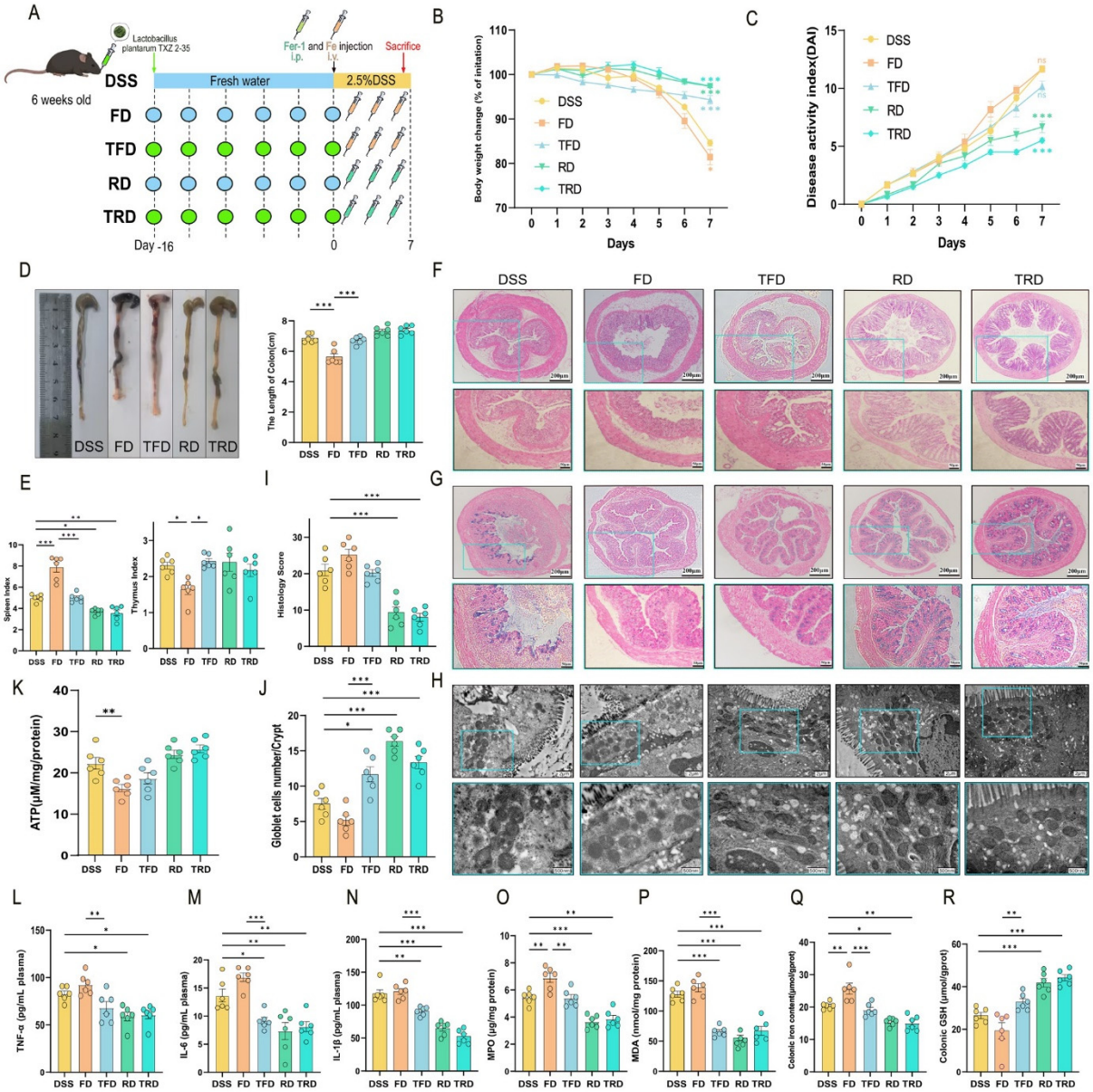

Fig 3 Inhibition of ferroptosis alleviated experimental colitis in mice. (A) Experimental protocol of Fer-1, ferric citrate and probiotic intervention in DSS-induced colitis. (B) Percentage change in body weight (%) across different groups.(C) DAI scores for all groups. Statistical significance was determined using two-way ANOVA, followed by Tukey test. *P≤0.05, **P≤0.01, ***P≤0.001 is FD, TFD, RD and TRD relative to DSS group. (D) Macroscopic observation (left) and colon length(right) on the final day. (E) Ratios of spleen weight to body weight (top) and thymus weight to body weight (bottom). (F) Representative images of H&E staining (left) and histology score (right) of colon tissues. (G) Representative images of Alcian blue staining (left) and goblet cell number (right) of colon tissues (scale bar: 500 μm and 50 μm). (H) Representative images of transmission electron micrographs of colonic epithelial cells (scale bar: 500 μm and 50 μm). (I) Histology scores , (J) Goblet cell number (K) and ATP levels in the colon tissues. (L) Serum levels of TNF-α, (M) IL-1β and (N) IL-6. (O) Concentration of MPO, (P) MDA, (Q)iron and (R) GSH in colon tissues. Data were shown as mean ± SEM. Statistical significance was determined using one-way ANOVA, followed by Tukey test. ns. not significant, *$P < 0.05$, **$P < 0.01$, ***$P < 0.001$.

3.4 L. plantarum TXZ 2-35 reverses gut dysbiosis in DSS-induced mice colitis

We conducted in vitro experiments using *L. plantarum* TXZ 2-35 and H1299 cells, which are commonly used in lipid peroxidation and ferroptosis research. The results indicated that TXZ 2-35 did not

significantly reduce ferroptosis in vitro(**Fig. S4**). Therefore, we speculate that Lactobacillus plantarum exerts its effects through mechanisms other than direct interaction with cells. Previous studies have indicated that gut microbial dysbiosis, along with specific, plays a crucial role in triggering ferroptosis[33-34]. Thus, the impact of TXZ 2-35 on the gut microbiota composition of colitis mice was investigated via 16S rRNA gene sequencing of the mice's stool samples. The OTU numbers in the three groups are listed in **Table S1**. The rarefaction curve and rank-abundance curve indicated that the sequencing depth and effective data rate met the requirements for subsequent analysis (**Fig. S2A,B**). The DSS group exhibited reduced α-diversity compared to the control group, whereas TXZ 2-35 increased the bacterial richness and diversity (**Fig. 4A**). In addition, NMDS result showed that the gut microbiota in DSS-treated mice was separated away from that of mice in the control group, while TXZ 2-35 treatments trended to shift the gut microbiota pattern from one more similar to the DSS group to that of the control group, while the changes were not identical (**Fig. 4B**). The overall fecal microbiota comprised nine main phyla, including *Firmicutes*, *Bacteroidetes*, *Proteobacteria*, *Verrucomicrobia*, *Tenericutes*, *Actinobacteria*, *Cyanobacteria*, *Deferribacteres* and *Patescibacteria*. In terms of bacterial composition at the phylum level, all samples shared similar taxonomic communities and exhibited a relatively high abundance of the phyla *Firmicutes* and *Bacteroidetes* (**Fig. 4C**). Interestingly, significant difference was found in the *Firmicutes* and *Bacteroidetes* between the Con and DSS group, while there were no significant difference in DSS and TD group (**Fig. S2C**). At the genus level, *Allobaculum*, *Ruminococcaceae_UCG-014*, *Lachnospiraceae_NK4A136_group*, *Lactobacillus* and *Bacteroides* were predominant genus in the fecal microbiota (**Fig. 4D**). Furthermore, to confirm which genus of bacterium were altered by TXZ 2-35 treatment, the differential genus between the Con, DSS and TD groups were analyzed by STAMP (**Fig. 4E**). Specifically, 8 and 12 differential genera were identified between the Con and DSS, DSS and TD groups, respectively. Notably, *Dubosiella* was more abundant in DSS group than Con or TD group, respectively. In addition, the DSS group had more *Bacteroides* and *Dubosiella*, less *Lactobacillus and Muribaculum* compared with the Con group, while the TD group had significantly more *Ruminococcus_1*, *Lachnospiraceae_NK4A136_group* and *Anaeroplasma,* less *Dubosiella* compared with the DSS group (**Fig. 4F**). These findings indicate a superior regulatory effect of TXZ 2-35 on gut microbiota composition and relative abundances of genera.

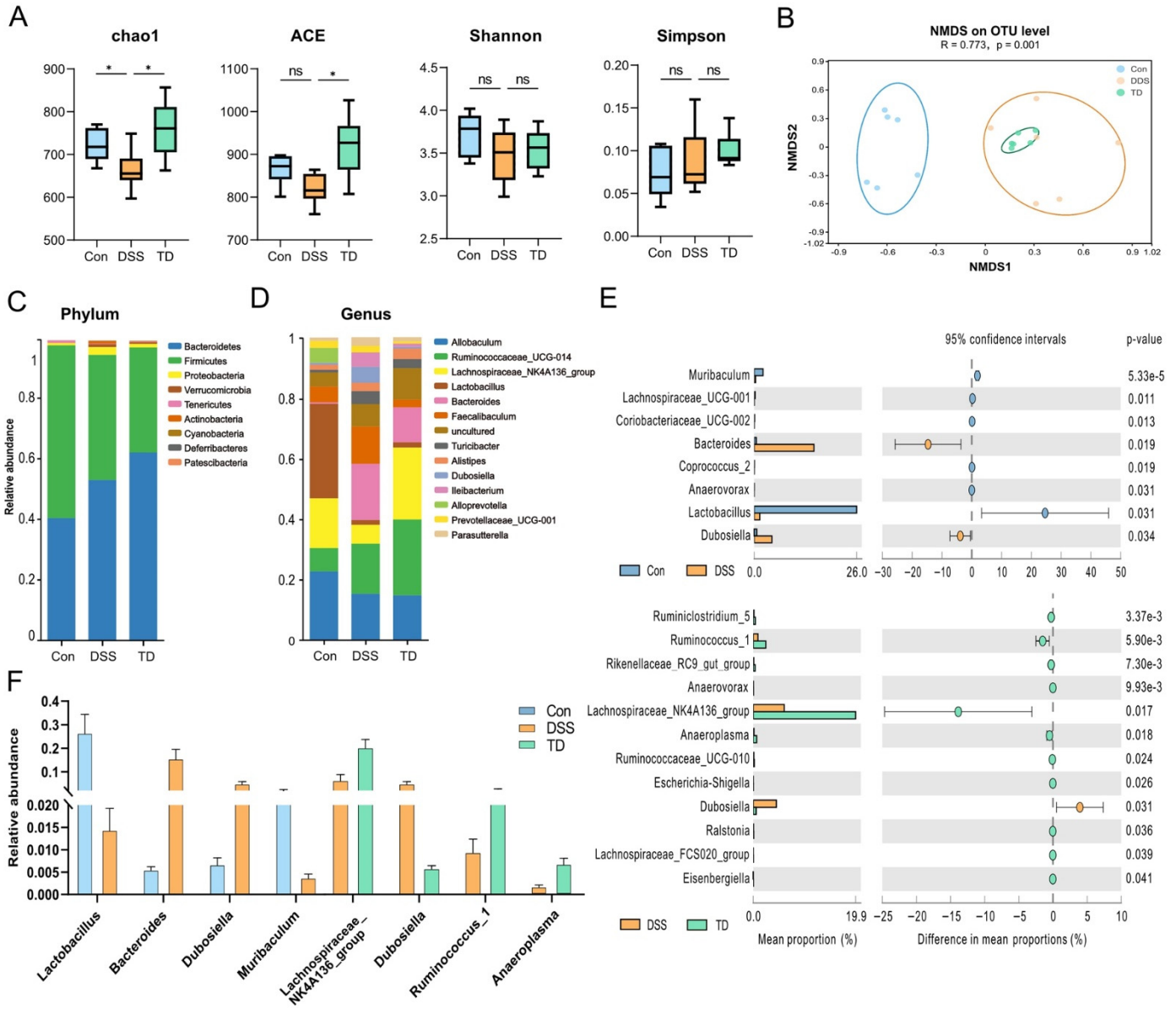

Fig 4 Modulation of the gut microbiome by *L. plantarum* TXZ 2-35 in DSS-induced mice colitis. (A)Alpha diversity of mice fecal bacteria in all groups. (B) Weighted UniFrac distance metrics of NMDS analysis at the OTU level. (C)Phylum-level gut microbiota profile. (D) genus-level gut microbiota profile. (E) Differential genus of three pairwise comparisons between Con, DSS and TD groups. (F) All three groups at the genus level, all genus showed significantly different using the Welch's t-test of STAMP.

3.5 L.plantarum TXZ 2-35 modulated gut lipidic metabolites in DSS-induced mice colitis

Lipid metabolites play critical roles in the development and regulation of ferroptosis. Their regulation is crucial for maintaining cellular homeostasis and preventing the initiation of ferroptosis, which has significant implications for a range of diseases including inflammatory conditions[35]. Thus, the impact of *L.plantarum* TXZ 2-35 on the gut microbial lipid metabolites were measured in DSS-induced colitis mice by LC-MS/MS. A total of 667 annotated metabolites, classified to five categories Phosphatidyl cholines (PC), Phosphatidyl ethanolamines (PE), Phosphatidylglycerol (PG) (**Fig. 5A**), were detected from feces samples. The lipid chains were classified according to their degree of unsaturation, specifically, SFA accounts for 23.4286%, MUFA accounts for 16.2857%, PUFA accounts for 30.2857% (**Fig. 5B**). Score plots of OPLS-DA constructed on the fecal metabolites separated the TD group from the DSS group, which

indicated a significant change in the DSS-induced colitis mice when they were supplemented with TXZ 2-35 (**Fig. 5C**). A total of 79 fecal metabolites differed between DSS and TD, including 18 upregulated metabolites and 61downregulated metabolites [(FC)≥1 or≤1, VIP>1, and P≤0.05] (**Fig. 5D**). Fecal lipid metabolomics pathway analysis based on differential metabolites showed the enrichment of "Sphingolipid metabolism" and "Glycerophospholipid metabolism" were the significantly different pathways ($P < 0.05$, **Fig. S3A**). The relative abundance of three class, which were Phosphatidyl cholines (PC), Phosphatidyl ethanolamines (PE), Phosphatidylglycerol (PG) affiliated to Glycerol phospholipid category were depicted in **Fig. 5E**, when compared to the DSS mice. Most PC, PE, PG were downregulated except for PG(16:0/16:0) and PG(4:0/18:1) in the pretreatment of TXZ 2-35. Interestingly, PL-PUFAs were all significantly decreased in TD group, compared with the DSS group (**Fig. 5F**). The ROC curve of these PL-PUFAs was shown in **Fig. S3B**. A correlation analysis was performed to explore the relationship between mice gut microbiota and fecal lipid metabolites. As shown in **Fig. 5G**,in the comparison of TD vs DSS, Dubosiella showed significant positive correlation with PE(15:0/18:2) and PE(15:0/20:4), negative with PG(4:0/18:1). Anaerovorax and Lachnospiraceae_FCS020_group showed significant negative with PL-PUFAs.

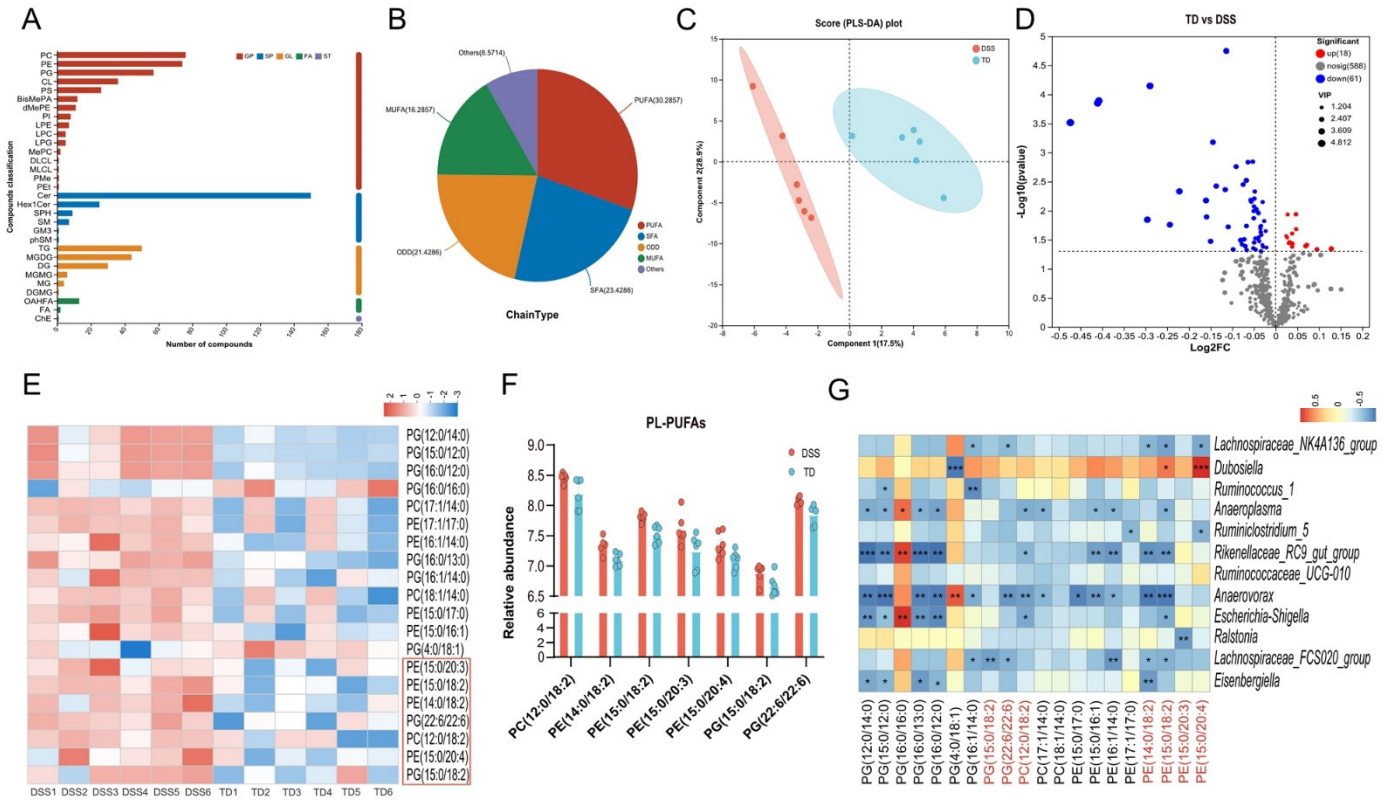

Fig 5 Lipids metabolites identified in the feces of DSS and TD groups. (A) Classification of all lipid metabolites. (B) Degree of carbon chain unsaturation in lipids metabolites. (C) OPLS-DA analysis displaying the grouped discrimination of DSS and TXZ 2-35 pretreatment. (D) Volcano plot of lipids between DSS and TD group mice feces. Blue dots indicate significantly decreased levels in the TD group, while red dots represent significantly increased levels. See also **Table S2**. (E) Heatmap of 20 differential lipids in PC, PE, PG class, the red box marked was PL-PUFAs. (F) The relative abundance of significantly altered PL-PUFAs in the TD group compared to DSS group. (G) Heatmap of Spearman's correlations between altered fecal microbes and fecal lipid metabolites, such as the font marked in red are PL-PUFAs.

4. Discussion

IBD is emerging as one of the health-threatening diseases all over the world. IBD prevalence was 321.2 per 100,000 population in 2021 and, compared with 2006 (200 per 100,000 population), the prevalence has increased at a rate of 46%[36]. Hence, there remains an urgent need for the development of effective and safe therapeutic methods. Probiotics have arisen the attention due to their effectiveness and safety, it is worth promoting them as an attractive treatment alternative for UC patients. *Bifidobacterium* and *Lactobacillus* are recommended as adjuvant therapy in China for adults with mild-to-moderate UC to maintain remission[37].

Probiotic-assisted therapy has been shown to be effective in preventing the recurrence of ulcerative colitis (UC) in patients in clinical remission, without increasing the risk of treatment-related adverse events[38-39]. Various probiotics have demonstrated different levels of protective effects against UC. For example, *Lactobacillus rhamnosus* GG has been reported to reduce inflammation and improve colonic histology in colitis models[40-41]. Similarly, *Bifidobacterium* has shown efficacy in reducing disease severity and modulating the immune response in UC patients[42-43]. In this study, we aimed to explore the therapeutic potential of *L.plantarum* TXZ 2-35 in treating colitis. Mice were pretreated with TXZ 2-35 or saline for 16 consecutive days, followed by the induction of acute colitis using 2.5% DSS. Consistent with previous studies[44-45]. TXZ 2-35 supplementation resulted in significant alleviation of DSS-induced colitis. This was evidenced by a decreased Disease Activity Index (DAI), reduced spleen index, and mitigated histological damage, increased colon length, higher number of goblet cells, as well as decreased level of inflammatory cytokines. Our results demonstrated that TXZ 2-35 significantly reduced inflammatory cytokines in colitis mice. Additionally, TXZ 2-35 supplementation improved histopathological manifestations of colitis, such as mucosal integrity and inflammation. These findings highlight the potential of TXZ 2-35 as a promising therapeutic agent for UC. Further studies are needed to understand the underlying mechanisms and evaluate the long-term efficacy and safety of TXZ 2-35 in clinical settings.

Ferroptosis is an iron-dependent form of regulated cell death characterized by the accumulation of lipid peroxides and oxidative stress[46]. Ample evidences have depicted an essential role for ferroptosis as either the cause or consequence for IBD, denoting the likely therapeutic promises for targeting ferroptosis in the preservation of human health[47-49]. Previous study has revealed that ferroptosis as a key regulatory mechanism in IBD[50], and inhibition of ferroptosis is expected to be a new direction in the prevention and treatment of IBD. Ferroptosis is closely related to changes in mitochondria, as it often involves mitochondrial dysfunction, including alterations in membrane integrity, reduced mitochondrial cristae, and increased oxidative stress, which contribute to the initiation and progression of this form of cell death[51-52]. In this study, we observed that the mitochondria with increased mitochondrial membrane density and vanishing of mitochondrial cristae in DSS group, while the pretreatment with TXZ 2-35 protected the reduction or vanishing of mitochondrial cristae. Moreover, pretreatment with TXZ 2-35 significantly attenuated DSS-induced accumulation of lipid peroxidation products MDA in the colon, increased the

synthesis of antioxidant enzymes GSH and decreased the iron level in the colon. Above data demonstrated that *L.plantarum* TXZ 2-35 attenuated the development of DSS-induced colitis by inhibiting ferroptosis.

In this study, we demonstrated that TXZ 2-35 effectively suppressed the effects of ferric citrate by reducing ferroptosis. Notably, combining TXZ 2-35 with Fer-1 did not enhance the therapeutic effects, as both treatments target the same ferroptosis pathway, confirming that ferroptosis is the primary mechanism of action for TXZ 2-35. While targeting ferroptosis by probiotics holds promise for treating various diseases, the underlying mechanisms are strain-specific. For instance, Zhang et al. reported that the oral administration of probiotics ameliorated benzene-induced hematopoietic toxicity in mice by modulating the Bacteroidaceae-intestinal ferroptosis-inflammation axis[53]. Similarly, it has been reported that the eukaryotic probiotic *Saccharomyces boulardii* attenuates cardiopulmonary bypass-induced acute lung injury by inhibiting ferroptosis[54]. *Acinetobacter baumannii* causes inflammatory damage to the respiratory tract through ferroptosis, while *Streptococcus* strain D19T inhibits the growth of *Acinetobacter baumannii* and reverses the inflammatory damage[55]. The inhibition of ferroptosis by probiotics may not occur through direct action (Fig. S4), as gut microbiota metabolites seem to play a more direct role in regulating ferroptosis in the gut. For instance, previous studies have demonstrated that the gut microbiota metabolite capsiate enhances Gpx4 expression and inhibits ferroptosis by activating TRPV1 in intestinal ischemia/reperfusion injury[56]. The microbiome-derived metabolite 3-HPAA facilitates spermatogenesis in aged mice through a ferroptosis-mediated mechanism by upregulating GPX4 expression[57]. Additionally, Lactobacillus paracasei and its exopolysaccharides have been shown to alleviate colon cancer cell growth (HT-29 and HCT-116) primarily by inducing apoptosis rather than ferroptosis[58]. These findings underscore the complexity and specificity of the mechanisms through which different probiotic strains exert their therapeutic effects, highlighting the importance of understanding strain-specific actions to develop effective treatments.

Intestinal microecology has recently gained significant attention for its role in both causing and alleviating various diseases. Notably, the gut microbiota can regulate ferroptosis, through its microbial composition, biological functions, and produced metabolites[59]. Our results indicated that *Ruminococcus*_1, *Lachnospiraceae*_NK4A136_group, *Anaeroplasma* were enriched and *Dubosiella* was decreased by TXZ 2-35 treatment compared with DSS group. Similarly, previous studies have revealed that DSS leads to the increase of *Dubosiella*[60-61]. In addition, the key microorganisms, including *Lachnospiraceae*_NK4A136_group and *Ruminococcus*_1, *Anaeroplasma* had a potential role in regulating colonic inflammation[62-63]. Although these structural changes in the gut microbiota were evident, whether these key microflora are responsible for the reduced ferroptosis observed with TXZ 2-35 treatment requires further investigation.

The gut microbiota has been shown to affect lipid metabolism and lipid levels in blood and tissues, both in mice and humans[64]. Specific classes of microbiota metabolites, notably bile acids, short-chain fatty acids, tryptophan metabolites and lipid metabolites, have been implicated in the pathogenesis of IBD[65]. Recent studies have shown that the metabolites produced by gut microbiota can exert regulatory effects by

influencing the occurrence and development of ferroptosis, such as annotating *Bacteroides sphingolipids* in an IBD metabolomic dataset revealed lower abundances in IBD and negative correlations with inflammation and host sphingolipid production[66-67]. Given that lipid peroxides are critical factors in the process of ferroptosis, we focused our investigation on lipid products derived from the gut microbiota. To comprehensively understand the influence of TXZ 2-35 pretreatment on lipid metabolites in mice, we employed an untargeted lipidomics approach. Interestingly, the PL-PUFAs were all significantly decreased in the TD group, compared with the DSS group. High amounts of PL-PUFAs are considered the driving force behind ferroptosis[12],[68]. Under oxidative or energetic stress, PUFA, particularly arachidonoyl (AA) and adrenic acid (AdA), is catalyzed by acyl-CoA synthetase long-chain family member 4 (ACSL4), lysophosphatidylcholine acyltransferase (LPCAT), and 15-lipoxygenase (15-LOX/ALOX15) to generate PUFA-containing phospholipids and induce ferroptosis to maintain redox homeostasis[69]. Similarly, it has been reported that PC-PUFA$_2$s induce mitochondrial ROS production essential for ferroptosis[70]. These findings underscore the *L.plantarum* TXZ 2-35 strain inhibited ferroptosis by modulating the gut lipidic metabolites PL-PUFAs.

5. Conclusion

In conclusion, our study demonstrates that *L. plantarum* TXZ 2-35 effectively mitigates DSS-induced colitis in mice by modulating the gut microbiota and reducing ferroptosis. The treatment enriched beneficial bacterial groups such as *Ruminococcus*_1, *Lachnospiraceae*_NK4A136_group, and *Anaeroplasma*, while decreasing the abundance of *Dubosiella*. These microbial changes were associated with improved colonic health and reduced inflammation. Additionally, our untargeted lipidomics analysis revealed significant alterations in lipid metabolites, underscoring the role of lipid peroxides in ferroptosis and highlighting the regulatory potential of microbiota-derived lipid products. Although our findings suggest that TXZ 2-35 can suppress ferroptosis and alleviate colitis, further research is needed to elucidate the specific mechanisms and to evaluate its long-term efficacy and safety. These results pave the way for developing TXZ 2-35 as a promising therapeutic agent for ulcerative colitis and other ferroptosis-related diseases.

Conflicts of interest

The authors have declared no competing interests.

Data availability

All the relevant data which support our findings are available from the authors on reasonable request; some have already been included in the paper and the supplemental material. Raw sequence data of microbiota which support the findings in our study have been deposited into NCBI's Sequence Read Archive under accession number PRJNA1138806. Raw sequence data of transcriptome that support our findings have been deposited in NCBI's Sequence Read Archive under accession number PRJNA1132914.

Acknowledgments

This study was funded by National Natural Science Foundation of China (No.32272297), Xianyang City's Major Science and Technology Innovation Special Plan (L2024-ZDKJ-ZDCGZH-0001) and the Key Research and Development Program of Shaanxi Province (2024NC-ZDCYL-03-09). We also acknowledge the sequencing supports from Biomarker Technologies Co., Ltd (Beijing, China) and lipidomic supports from Majorbio Bio-pharm Technology Co.,Ltd (Shanghai, China).

Reference

[1] M. H. Geukes Foppen, E. A. Rozeman, S. van Wilpe, et al. Immune checkpoint inhibition-related colitis: symptoms, endoscopic features, histology and response to management.ESMO Open,3 (1) (2018), https://doi.org/10.1136/esmoopen-2017-000278.

[2] S. C. Shah, S. H. Itzkowitz. Colorectal Cancer in Inflammatory Bowel Disease: Mechanisms and Management. Gastroenterology,162 (3) (2022), pp. 715-730, https://doi.org/10.1053/j.gastro.2021.10.035.

[3] M. Agrawal, K. H. Allin, F. Petralia, et al. Multiomics to elucidate inflammatory bowel disease risk factors and pathways. Nat. Rev. Gastroenterol. Hepatol.,19 (6) (2022), pp.399-409, https://doi.org/10.1038/s41575-022-00593-y.

[4] Y. Hu, Z. Chen, C. Xu, et al. Disturbances of the Gut Microbiota and Microbiota-Derived Metabolites in Inflammatory Bowel Disease. Nutrients, 14 (23) (2022), https://doi.org/10.3390/nu14235140.

[5] N. A. Khalil, N. A. Alfaris, J. Z. Altamimi, et al. Anti-inflammatory effects of bay laurel (Laurus nobilis L.) towards the gut microbiome in dextran sodium sulfate induced colitis animal models. Food Sci. Nutr., 12 (4) (2024), pp.2650-2660,https://doi.org/10.1002/fsn3.3946.

[6] X.-F. Zhang, X.-X. Guan, Y.-J. Tang,et al. Clinical effects and gut microbiota changes of using probiotics, prebiotics or synbiotics in inflammatory bowel disease: a systematic review and meta-analysis. Eur. J. Nutr.,60 (5) (2021), pp.2855-2875, https://doi.org/10.1007/s00394-021-02503-5.

[7] V. D. Bamola, D. Dubey, P. Samanta, et al. Role of a probiotic strain in the modulation of gut microbiota and cytokines in inflammatory bowel disease. Anaerobe,78 (2022), https://doi.org/10.1016/j.anaerobe.2022.102652.

[8] S. Sun, J. Shen, J. Jiang, et al. Targeting ferroptosis opens new avenues for the development of novel therapeutics. Signal Transduct. Target. Ther., 8 (1) (2023), https://doi.org/10.1038/s41392-023-01606-1.

[9] R. Qian, M. Tang, Z. Ouyang, et al. Identification of ferroptosis-related genes in ulcerative colitis: a diagnostic model with machine learning. Ann. Transl. Med.,11 (4) (2023), pp.177-177, https://doi.org/10.21037/atm-23-276.

[10] M. Xu, J. Tao, Y. Yang, et al. Ferroptosis involves in intestinal epithelial cell death in ulcerative colitis. Cell Death Dis., 11 (2) (2020), pp.86 , https://doi.org/10.1038/s41419-020-2299-1.

[11] J. V. Patankar , C. Becker. Cell death in the gut epithelium and implications for chronic inflammation. Nat. Rev. Gastroenterol. Hepatol., 17 (9) (2020), pp.543-556 , https://doi.org/10.1038/s41575-020-0326-4.

[12] J. Lee, D. Shin , J.-L. Roh. Lipid metabolism alterations and ferroptosis in cancer: Paving the way for solving cancer resistance. Eur. J. Pharmacol., (2023), pp.941, https://doi.org/10.1016/j.ejphar.2023.175497.

[13] W. Cui, M. Guo, D. Liu, et al. Gut microbial metabolite facilitates colorectal cancer development via ferroptosis inhibition. Nat. Cell Biol., 26 (1) (2024), pp.124-137, https://doi.org/10.1038/s41556-023-01314-6.

[14] Y. Zeng, R. Wu, F. Wang, et al. Liberation of daidzein by gut microbial beta-galactosidase suppresses acetaminophen-induced hepatotoxicity in mice. Cell Host Microbe, 31 (5) (2023), pp.766-780, https://doi.org/10.1016/j.chom.2023.04.002.

[15] P. Kong, M. Yang, Y. Wang, et al. Ferroptosis triggered by STAT1- IRF1-ACSL4 pathway was involved in radiation-induced intestinal injury. Redox Biol., (2023), pp.66, https://doi.org/10.1016/j.redox.2023.102857.

[16] S. Liu, Z. Gao, W. He, et al. The gut microbiota metabolite glycochenodeoxycholate activates TFR-ACSL4-mediated ferroptosis to promote the development of environmental toxin-linked MAFLD. Free Radic. Biol. Med., 193 (Pt 1) (2022) , pp.213-226, https://doi.org/10.1016/j.freeradbiomed.2022.10.270.

[17] M. S. Mortensen, J. Ruiz, J. L. Watts. Polyunsaturated Fatty Acids Drive Lipid Peroxidation during Ferroptosis. Cells, 12 (5) (2023), https://doi.org/10.3390/cells12050804.

[18] B. A. Tegegne, B. Kebede. Probiotics, their prophylactic and therapeutic applications in human health development: A review of the literature. Heliyon, 8 (6) (2022), https://doi.org/ 10.1016/j.heliyon.2022.e09725.

[19] D. Liu, F. Zhao, L. Li, et al. Enhancing the antioxidant capacity and quality attributes of fermented goat milk through the synergistic action of Limosilactobacillus fermentum WXZ 2-1 with a starter culture. Journal of Dairy Science, 107(4),(2024), 1928-1949, https://doi.org/10.3168/jds.2023-24135.

[20] G. Wang, S. Qin, Y. Zheng, et al. T-2 Toxin Induces Ferroptosis by Increasing Lipid Reactive Oxygen Species (ROS) and Downregulating Solute Carrier Family 7 Member 11 (SLC7A11). Journal of agricultural and food chemistry, 69(51), (2021) , 15716–15727. https://doi.org/10.1021/acs.jafc.1c05393.

[21] C. Li, G. Ai, Y. Wang, et al. Oxyberberine, a novel gut microbiota-mediated metabolite of berberine, possesses superior anti-colitis effect: Impact on intestinal epithelial barrier, gut microbiota profile and TLR4-MyD88-NF-kappaB pathway. Pharmacol. Res., 152 (2020), pp.104603, https://doi.org/ 10.1016/j.phrs.2019.104603.

[22] H. Lu, M. Shen, Y. Chen, et al. Alleviative effects of natural plant polysaccharides against DSS-induced ulcerative colitis via inhibiting inflammation and modulating gut microbiota. Food Res. Int., 167 (2023), pp.112630, https://doi.org/10.1016/j.foodres.2023.112630.

[23] J. Li, K. Lu, F. Sun, et al. Panaxydol attenuates ferroptosis against LPS-induced acute lung injury in mice by Keap1-Nrf2/HO-1 pathway. J. Transl. Med., 19 (1) (2021),pp. 96, https://doi.org/10.1186/s12967-021-02745-1.

[24] Y. Yu, L. Jiang, H. Wang, et al. Hepatic transferrin plays a role in systemic iron homeostasis and liver ferroptosis. Blood, 136(6) (2020),pp.726-739, https://doi.org/10.1182/blood.2019002907

[25] R. Caruso, T. Mathes, E. C. Martens, et al. A specific gene-microbe interaction drives the development of Crohn's disease-like colitis in mice. Sci. Immunol., 4 (34) (2019), https://doi.org/10.1126/sciimmunol.aaw4341.

[26] M. I. Love, W. Huber, S. Anders. Moderated estimation of fold change and dispersion for RNA-seq data with DESeq2. Genome Biol., 15 (2014), pp.550, https://doi.org/10.1186/s13059-014-0550-8.

[27] C. Yang, D. Merlin. Unveiling Colitis: A Journey through the Dextran Sodium Sulfate-induced Model. Inflamm. Bowel Dis., 30 (5) (2024), pp. 844-853, https://doi.org/10.1093/ibd/izad312.

[28] K. Gu, A. Wu, B. Yu, et al. Iron overload induces colitis by modulating ferroptosis and interfering gut microbiota in mice. Sci. Total Environ., (2023), pp.905, https://doi.org/10.1016/j.scitotenv.2023.167043.

[29] A. Yokote, N. Imazu, J. Umeno, et al. Ferroptosis in the colon epithelial cells as a therapeutic target for ulcerative colitis. J. Gastroenterol., 58 (9) (2023), pp.868-882, https://doi.org/ 10.1007/s00535-023-02016-4.

[30] L. Shen, J. Zhang, Z. Zheng, et al. PHGDH Inhibits Ferroptosis and Promotes Malignant Progression by Upregulating SLC7A11 in Bladder Cancer. Int. J. Biol. Sci., 18 (14) (2022), pp.5459-5474, https://doi.org/10.7150/ijbs.74546.

[31] H. Wu, Q. Liu, X. Shan, et al. ATM orchestrates ferritinophagy and ferroptosis by phosphorylating NCOA4. Autophagy, 19 (7) (2023), pp. 2062-2077, https://doi.org/10.1080/15548627.2023.2170960.

[32] X. Zhu, L. Wang, K. Wang, et al. Erdafitinib promotes ferroptosis in human uveal melanoma by inducing ferritinophagy and lysosome biogenesis via modulating the FGFR1/mTORC1/TFEB signaling axis. Free Radic. Biol. Med., 222 (2024), pp.552-568, https://doi.org/10.1016/j.freeradbiomed.2024.07.002.

[33]A. E. V. Quaglio, T. G. Grillo, E. C. S. D. Oliveira, et al. Gut microbiota, inflammatory bowel disease and colorectal cancer. World J. Gastroenterol.,28 (30) (2022), pp.4053-4060, https://doi.org/10.3748/wjg.v28.i30.4053.

[34] C. Wang, Q. Chu, W. Dong, et al. Microbial metabolite deoxycholic acid-mediated ferroptosis exacerbates high-fat diet-induced colonic inflammation. Mol. Metab., (2024), pp.84, https://doi.org/10.1016/j.molmet.2024.101944.

[35] L. E. Pope, S. J. Dixon. Regulation of ferroptosis by lipid metabolism. Trends Cell Biol., 33 (12) (2023), pp.1077-1087, https://doi.org/10.1016/j.tcb.2023.05.003.

[36] G. P. Caviglia, A. Garrone, C. Bertolino, et al. Epidemiology of Inflammatory Bowel Diseases: A Population Study in a Healthcare District of North-West Italy. J. Clin. Med., 12 (2) (2023), https://doi.org/ 10.3390/jcm12020641.

[37] C. Huang, W. Hao, X. Wang, et al. Probiotics for the treatment of ulcerative colitis: a review of experimental research from 2018 to 2022. Front. Microbiol., 14 (2023), pp.1211271, https://doi.org/10.3389/fmicb.2023.1211271.

[38] W. Jin, H. Ai, Q. Huang, et al. Preclinical evidence of probiotics in ulcerative colitis: a systematic review and network meta-analysis. Front. Pharmacol., 14 (2023), pp.1187911, https://doi.org/10.3389/fphar.2023.1187911.

[39] C. Wang, C. Zhou, S. Zhang, et al. Additive efficacy and safety of probiotics in the treatment of ulcerative colitis: a systematic review and meta-analysis. Eur. J. Nutr., (2024), https://doi.org/10.1007/s00394-023-03307-5.

[40] D. Chen, H. Tang, Y. Li, et al. Vitamin D3 andLactobacillus rhamnosusGG/p40 Synergize to Protect Mice From Colitis by Promoting Vitamin D Receptor Expression and Epithelial Proliferation. Inflamm. Bowel Dis., 29 (4) (2023), pp.620-632, https://doi.org/10.1093/ibd/izac238.

[41] C. Pagnini, M. C. Di Paolo, R. Urgesi, et al. Safety and Potential Role of Lactobacillus rhamnosus GG Administration as Monotherapy in Ulcerative Colitis Patients with Mild–Moderate Clinical Activity. Microorganisms, 11 (6) (2023), https://doi.org/10.3390/microorganisms11061381.

[42] Furrie, E. Synbiotic therapy (Bifidobacterium longum/Synergy 1) initiates resolution of inflammation in patients with active ulcerative colitis: a randomised controlled pilot trial. Gut, 54 (2) (2005), pp.242-249, https://doi.org/10.1136/gut.2004.044834.

[43] G. Leccese, A. Bibi, S. Mazza, et al. Probiotic Lactobacillus and Bifidobacterium Strains Counteract Adherent-Invasive Escherichia coli (AIEC) Virulence and Hamper IL-23/Th17 Axis in Ulcerative Colitis, but Not in Crohn's Disease. Cells, 9 (8) (2020), https://doi.org/10.3390/cells9081824.

[44] I. Khan, J. Wei, A. Li, et al. Lactobacillus plantarum strains attenuated DSS-induced colitis in mice by modulating the gut microbiota and immune response. Int. Microbiol., 25 (3) (2022), pp.587-603, https://doi.org/10.1007/s10123-022-00243-y.

[45] H.-J. Kim, H.-J. Jeon, J.-Y. Kim, et al. Lactiplantibacillus plantarum HY7718 Improves Intestinal Integrity in a DSS-Induced Ulcerative Colitis Mouse Model by Suppressing Inflammation through Modulation of the Gut Microbiota. Int. J. Mol. Sci.,25 (1) (2024), https://doi.org/10.3390/ijms25010575.

[46] S. Doll, B. Proneth, Y. Y. Tyurina, et al.ACSL4 dictates ferroptosis sensitivity by shaping cellular lipid composition. Nat. Chem. Biol.,13 (1) (2017), pp.91-98, https://doi.org/10.1038/nchembio.2239.

[47] J. Huang, J. Zhang, J. Ma, et al. Inhibiting Ferroptosis: A Novel Approach for Ulcerative Colitis Therapeutics. Oxid. Med. Cell. Longev., (2022), pp.1-9, https://doi.org/10.1155/2022/9678625.

[48] L. Luo, S. Zhang, N. Guo, et al. ACSF2-mediated ferroptosis is involved in ulcerative colitis. Life Sci., (2023), pp.313, https://doi.org/10.1016/j.lfs.2022.121272.

[49] R. Ren, A. Q. Zhao, L. Chen, et al. Therapeutic effect of Lactobacillus plantarum JS19 on mice with dextran sulfate sodium induced acute and chronic ulcerative colitis. J. Sci. Food Agric., 103 (8) (2023), pp.4143-4156, https://doi.org/10.1002/jsfa.12414.

[50] J. Huang, J. Zhang, J. Ma, et al. Inhibiting Ferroptosis: A Novel Approach for Ulcerative Colitis Therapeutics. Oxid. Med. Cell. Longev., (2022), pp.9678625, https://doi.org/10.1155/2022/9678625.

[51] S. J. Dixon, J. A. Olzmann. The cell biology of ferroptosis. Nat. Rev. Mol. Cell Biol., 25 (6) (2024), pp.424-442, https://doi.org/10.1038/s41580-024-00703-5.

[52] JX. Jiang, B. R. Stockwell, M. Conrad. Ferroptosis: mechanisms, biology and role in disease. Nat. Rev. Mol. Cell Biol., 22 (4) (2021), pp.266-282, https://doi.org/10.1038/s41580-020-00324-8.

[53] L. Zhang, H. Kang, W. Zhang, et al. A. Probiotics ameliorate benzene-induced systemic inflammation and hematopoietic toxicity by inhibiting Bacteroidaceae-mediated ferroptosis. Sci. Total Environ., 899 (2023), pp.165678, https://doi.org/10.1016/j.scitotenv.2023.165678.

[54] J. Li, P.-F. Gao, Y.-X. Xu, et al. Probiotic Saccharomyces boulardii attenuates cardiopulmonary bypass-induced acute lung injury by inhibiting ferroptosis. Am. J. Transl. Res., 14(7) (2022),pp.5003-5013.

[55] Y. Sun, S. Li, Y. Che, et al. A respiratory Streptococcus strain inhibits Acinetobacter baumannii from causing inflammatory damage through ferroptosis. BMC microbiology, 24(1), (2024), 437, https://doi.org/10.1186/s12866-024-03589-7.

[56] F. Deng, B. C. Zhao, X. Yang, et al. The gut microbiota metabolite capsiate promotes Gpx4 expression by activating TRPV1 to inhibit intestinal ischemia reperfusion-induced ferroptosis. Gut microbes, 13(1),(2021), 1–21. https://doi.org/10.1080/19490976.2021.1902719.

[57] Z. Jin, Y. Yang, Y. Cao, et al. The gut metabolite 3-hydroxyphenylacetic acid rejuvenates spermatogenic dysfunction in aged mice through GPX4-mediated ferroptosis. Microbiome, 11(1),(2023),212. https://doi.org/10.1186/s40168-023-01659-y.

[58] Y. Rahbar Saadat, B. Pourghassem Gargari, A. Shahabi, et al. Prophylactic Role of Lactobacillus paracasei Exopolysaccharides on Colon Cancer Cells through Apoptosis Not Ferroptosis. Pharm. Sci., 27 (2) (2020), pp. 251-261, https://doi.org/ 10.34172/ps.2020.39.

[59] T. Yao, L. Li. The influence of microbiota on ferroptosis in intestinal diseases. Gut Microbes, 15 (2) (2023), pp.2263210, https://doi.org/ 10.1080/19490976.2023.2263210.

[60] P. Feng, Q. Li, L. Liu, et al. Crocetin Prolongs Recovery Period of DSS-Induced Colitis via Altering Intestinal Microbiome and Increasing Intestinal Permeability. Int. J. Mol. Sci., 23 (7) (2022), https://doi.org/10.3390/ijms23073832.

[61] K. Wang, L. Qin, J. Cao, et al. κ-Selenocarrageenan Oligosaccharides Prepared by Deep-Sea Enzyme Alleviate Inflammatory Responses and Modulate Gut Microbiota in Ulcerative Colitis Mice. Int. J. Mol. Sci., 24 (5) (2023), https://doi.org/10.3390/ijms24054672.

[62] T. J. Gates, C. Yuan, M. Shetty, et al. Fecal Microbiota Restoration Modulates the Microbiome in Inflammation-Driven Colorectal Cancer. Cancers, 15 (8) (2023), https://doi.org/10.3390/cancers15082260.

[63] X. Shao, C. Sun, X. Tang, et al. Anti-Inflammatory and Intestinal Microbiota Modulation Properties of Jinxiang Garlic (Allium sativum L.) Polysaccharides toward Dextran Sodium Sulfate-Induced Colitis. J. Agric. Food Chem., 68 (44) (2020), pp.12295-12309, https://doi.org/10.1021/acs.jafc.0c04773.

[64] M. Schoeler, & R. Caesar. Dietary lipids, gut microbiota and lipid metabolism. Reviews in endocrine & metabolic disorders, 20(4), (2019), 461–472. https://doi.org/10.1007/s11154-019-09512-0.

[65] A. Lavelle, & H. Sokol. Gut microbiota-derived metabolites as key actors in inflammatory bowel disease. Nature reviews. Gastroenterology & hepatology, 17(4), (2020), 223–237, https://doi.org/10.1038/s41575-019-0258-z.

[66] E. M. Brown, J. Clardy, & R. J. Xavier. Gut microbiome lipid metabolism and its impact on host physiology. Cell host & microbe, 31(2), (2023),173–186, https://doi.org/10.1016/j.chom.2023.01.009.

[67] Eric M. Brown, et al. Bacteroides-Derived Sphingolipids Are Critical for Maintaining Intestinal Homeostasis and Symbiosis. Cell host & microbe, 25(5), (2019), 668-680, https://doi.org/10.1016/j.chom.2019.04.002.

[68] Z. H. Yuan, T. Liu, H. Wang, et al. Fatty Acids Metabolism: The Bridge Between Ferroptosis and Ionizing Radiation. Front. Cell Dev. Biol., 9 (2021), pp.675617, https://doi.org/ 10.3389/fcell.2021.675617.

[69] G. Lei, L. Zhuang, B. Gan. Targeting ferroptosis as a vulnerability in cancer. Nat. Rev. Cancer, 22 (7) (2022), pp.381-396, https://doi.org/ 10.1038/s41568-022-00459-0.

[70] B. Qiu, F. Zandkarimi, C. T. Bezjian, et al. Phospholipids with two polyunsaturated fatty acyl tails promote ferroptosis. Cell,187(5) (2024), pp.1177-1190.e18, https://doi.org/10.1016/j.cell.2024.01.030.